

**First Three-dimensional Actinide Polyrotaxane
Framework Mediated by Windmill-like Six-connected
Oligomeric Uranyl: Dual Roles of the Pseudorotaxane
Precursor**

Lei Mei,^a Zhen-ni Xie,^a Kong-qiu Hu,^a Lin Wang,^a Li-yong Yuan,^a Zi-jie Li,^a Zhi-fang Chai,^{ab} and

Wei-qun Shi*,^a

*E-mail: shiwq@ihep.ac.cn

*^aLaboratory of Nuclear Energy Chemistry and Key Laboratory for Biomedical Effects of
Nanomaterials and Nanosafety, Institute of High Energy Physics, Chinese Academy of Sciences,
Beijing 100049, China*

*^bSchool of Radiological and Interdisciplinary Sciences and Collaborative Innovation Center of
Radiation Medicine of Jiangsu Higher Education Institutions, Soochow University, Suzhou
215123, China*

Supplementary Information

Table of contents

S1. Synthesis and characterization

General Methods.

Preparation of **C4CN3** and **C4CN3@CB6** (L_1) ligands

Hydrothermal synthesis of **IHEP-URCP-1**, **IHEP-URCP-2** and **IHEP-URCP-3**

X-ray Single Crystal Structural Determination

S2. Typical Figures and Data

Figure S1. ^1H NMR spectrum of **C4CN3@CB6** (500 MHz in D_2O)

Figure S2. Crystallographic structure of **IHEP-URCP-2**: (a) ORTEP drawing of the asymmetric unit; (b) the asymmetric unit with all the cucurbituril macrocyclic moieties omitted for clarity.

Figure S3. Three types of **C4CA3@CB6** moieties in **IHEP-URCP-2**: **C4CA3@CB6** with both ends in η^1 -mode corresponds to type A, that in $\mu_2\text{-}\eta^1\text{:}\eta^1$ -mode is type B, and that in $\mu_2\text{-}\eta^1\text{:}\eta^2$ -mode is type C.

Figure S4. The α -polonium-like topology of the 3D uranyl polyrotaxane framework in **IHEP-URCP-2** viewed from different directions.

Figure S5. For 6-connected tetra-nuclear uranyl SBUs, all the six linkers extending to three different non-coplanar directions could afford three-dimensional frameworks, while those in coplanar directions only give 2D networks.

Figure S6. Top: (a) Free pseudorotaxane dicarboxylate molecules located in the well-defined cavity of 3D uranyl polyrotaxane framework; (b) with the cucurbituril macrocyclic moieties of 3D framework; (c) with all the cucurbituril macrocyclic moieties. Bottom: (d) Close view of the octahedral metal-organic rotaxane cavity with pseudorotaxane guest molecules. (e): with the cucurbituril macrocyclic moieties of 3D framework; (f): schematic diagram of the octahedral metal-organic rotaxane cavity.

Figure S7. Crystallographic structure of **IHEP-URCP-3**: (a) ORTEP drawing of the asymmetric unit; (b) the asymmetric unit with all the cucurbituril macrocyclic moieties omitted for clarity; (c) the chain-like structure of **IHEP-URCP-3**; (d) the chain-like structure of **IHEP-URCP-3** viewed from another direction.

Figure S8. Powder X-ray diffraction pattern (PXRD) of **IHEP-URCP-2**. The upper and lower parts are experimental spectrum and simulated spectrum based on single crystal data, respectively.

Figure S9. Powder X-ray diffraction pattern (PXRD) of **IHEP-URCP-3**. The upper and lower parts are experimental spectrum and simulated spectrum based on single crystal data, respectively.

Figure S10. Thermogravimetric results of **IHEP-URCP-2** and **IHEP-URCP-3**.

Figure S11. Fluorescence spectra of **IHEP-URCP-2** and **IHEP-URCP-3**.

Figure S12. IR spectra of **IHEP-URCP-2** and **IHEP-URCP-3**.

S1. Synthesis and characterization

General Methods.

Caution! Suitable measures for precautions and protection should be taken, and all operations should follow the criteria while handling such substances although natural uranium was used in the experiment. All the reagents were purchased from commercial sources and used as received. Cucurbit[6]uril (CB[6](HCl)) was synthesized from glycoluril and paraformaldehyde in HCl aqueous solution according to the reported procedure.¹⁻³

¹H-NMR spectra were recorded on a Bruker AVANCE III (500 MHz, Bruker, Switzerland) with deuterium oxide (D₂O) as a solvent. ESI-MS spectra were obtained with a Bruker AmaZon SL ion trap mass spectrometer (Bruker, USA). Powder XRD measurements (PXRD) were recorded on a Bruker D8 Advance diffractometer with Cu K α radiation ($\lambda=1.5406 \text{ \AA}$) in the range 5-80° (step size: 0.02°). Thermogravimetric analysis (TGA) was performed on a TA Q500 analyzer over the temperature range of 25-800 °C in air atmosphere with a heating rate of 10 °C/min. The Fourier transform infrared (IR) spectra were recorded from KBr pellets in the range of 4000-400 cm⁻¹ on a Bruker Tensor 27 spectrometer. Raman spectra were recorded from 4500 to 100 cm⁻¹ on a Horiba LabRAM HR Evolution Microscopic Confocal Raman spectrometer with a 473 nm argon ion laser. Solid-state fluorescence spectra of all the compounds were measured on a Hitachi F-4600 fluorescence spectrophotometer excited at 420 nm.

Preparation of C4CN3 and C4CN3@CB6 (L₁) ligands

C4CN3 was synthesized according to the procedures reported previously^{2,4} and **C4CN3@CB6 (L₁)** was also synthesized according to the procedures reported previously²⁻⁴.

C4CN3@CB6 (L₁): ¹H NMR (500MHz, D₂O, δ ppm): 8.25 (s, 2H); 8.14 (d, 2H), 7.93 (d, 2H), 7.73 (t, 2H), 5.77 (d, 12H), 5.74 (s, 12H), 4.48 (s, 4H), 4.42 (d, 4H), 2.54 (m, 4H), 0.66 (m, 4H). MS (ESI): mass calculated for C₅₆H₆₀N₂₈O₁₂ (M²⁺), 1316.50; m/z found, 658.21 (M²⁺).

Hydrothermal synthesis of IHEP-URCP-1, IHEP-URCP-2 and IHEP-URCP-3

IHEP-URCP-2: UO₂(NO₃)₂·6H₂O (0.5 mol/L, 18 μ L, 0.0090 mmol) were added to a suspension of L₁ (0.012 g, 0.083 mmol) in water (0.5 mL) in a stainless-steel bomb. After adjusting the initial pH to ~1.7 with HNO₃ (4 mol/L), the mixture was sealed, kept at 180°C for 72

h and cooled to room temperature to afford bright yellow block crystals. The final solution pH is ~2.3. The obtained crystals were washed with water and dried in air (9.5 mg, 64%).

IHEP-URCP-3: $\text{UO}_2(\text{NO}_3)_2 \cdot 6\text{H}_2\text{O}$ (0.5 mol/L, 18 μL , 0.0090 mmol) and $(\text{NH}_4)_2\text{SO}_4$ (0.5 mol/L, 18 μL , 0.0090 mmol) were added to a suspension of **L**₁ (0.012 g, 0.083 mmol) in water (0.5 mL) in a stainless-steel bomb. After adjusting the initial pH to ~1.6 with HNO_3 (4 mol/L), the mixture was sealed, kept at 180°C for 72 h and cooled to room temperature to afford prismatic yellow-green crystals. The final solution pH is ~2.1. The obtained crystals were washed with water and dried in air (11.2 mg, 72%).

IHEP-URCP-1: As a control compound, **IHEP-URCP-1** was synthesized according to the literature reported previously.² $\text{UO}_2(\text{NO}_3)_2 \cdot 6\text{H}_2\text{O}$ (140 μL , 0.07 mmol) were added to a suspension of **1** (0.10 g, 0.07 mmol) in water (2 mL) in a stainless-steel bomb. After treating with HNO_3 or triethylamine, the mixture was sealed, kept at 180°C for 72 h and cooled to room temperature. Light yellow crystals were washed with water and ethanol and dried in air.

X-ray Single Crystal Structural Determination

X-ray diffraction data for both the compounds **IHEP-URCP-2** and **IHEP-URCP-3** were collected on Agilent SuperNova X-ray CCD diffractometer with a Mo $K\alpha$ ($\lambda = 0.71073 \text{ \AA}$) X-ray source at 293 K. Standard Agilent CrysAlis software was used for determination of the unit cells and data collection control. The crystal structures were solved by means of direct methods and refined with full-matrix least squares on SHELXL-97. In both of the compounds, the unit cell includes a large region of disordered solvent water molecules, which could not be modeled as discrete atomic sites. We employed PLATON/SQUEEZE to produce a set of solvent-free diffraction intensities, which is used to make a further refinement. Crystallographic data for the structures in this paper have been deposited with the Cambridge Crystallographic Data Centre as supplementary publication nos. CCDC-1477807 (**IHEP-URCP-2**), CCDC-1477808 (**IHEP-URCP-3**).

Crystal data for **IHEP-URCP-2** (CCDC-1477807):

$\text{C}_{112}\text{H}_{121}\text{N}_{52}\text{O}_{38}\text{U}_2$, $[(\text{UO}_2)_2\text{O}(\text{C}_{20}\text{H}_{24}\text{N}_2\text{O}_4@CB6)_{1.5}(\text{H}_2\text{O})] \cdot (\text{C}_{20}\text{H}_{24}\text{N}_2\text{O}_4@CB6)_{0.5}$, Mr = 3279.67, triclinic, $P\bar{1}$, $a = 17.5238(6) \text{ \AA}$, $b = 21.4858(5) \text{ \AA}$, $c = 22.2555(7) \text{ \AA}$, $\alpha = 106.510(2)^\circ$, $\beta = 105.257(3)^\circ$, $\gamma = 105.879(2)^\circ$, $V = 7180.0(4) \text{ \AA}^3$, $Z = 2$, $\rho_{\text{calcd.}} = 1.517 \text{ g}\cdot\text{cm}^{-3}$. Of the 60006 reflections collected, 25250 were unique ($R_{\text{int}} = 0.0326$). Refinement on all data converged at $R_1 = 0.0434$ for 19821 reflections [$I > 2\sigma(I)$]. $wR_2 = 0.1229$, and GOF = 1.147.

Crystal data for **IHEP-URCP-3** (CCDC-1477808):

$\text{C}_{56}\text{H}_{60}\text{N}_{26}\text{O}_{22}\text{SU}$, $\text{UO}_2(\text{C}_{20}\text{H}_{24}\text{N}_2\text{O}_4@CB6)(\eta^2\text{-SO}_4)$. Mr = 1721.41, monoclinic, $P 2_1/n$, $a =$

16.5786(3) Å, $b = 16.9736(5)$ Å, $c = 25.6419(6)$ Å, $\beta = 101.461(2)^\circ$, $V = 7071.8(3)$ Å³, $Z = 4$, $\rho_{\text{calcd.}} = 1.615$ g•cm⁻³. Of the 29146 reflections collected, 13091 were unique ($R_{\text{int}} = 0.0400$). Refinement on all data converged at $R_1 = 0.0468$ for 10161 reflections [$I > 2\sigma(I)$]. $wR_2 = 0.1550$, and GOF = 1.056.

Reference

1. Day, A.; Arnold, A. P.; Blanch, R. J.; Snushall, B. *J. Org. Chem.*, **2001**, 66, 8094-8100.
2. Mei, L.; Wu, Q. Y.; Liu, C. M.; Zhao, Y. L.; Chai, Z. F.; Shi, W. Q., *Chem. Commun.* **2014**, 50, 3612-3615.
3. Mei, L.; Wang, L.; Yuan L. Y.; An, S. W.; Zhao, Y. L.; Chai, Z. F.; Burns, P. C.; Shi, W. Q., *Chem. Commun.* **2015**, 51, 11990-11993.
4. Kim, J.; Jung, In-S.; Kim, S. Y.; Lee, E.; Kang, J. K.; Sakamoto, S.; Yamaguchi, K. and Kim, K. *J. Am. Chem. Soc.*, **2000**, 122, 540-541.

S2. Typical Figures and Data

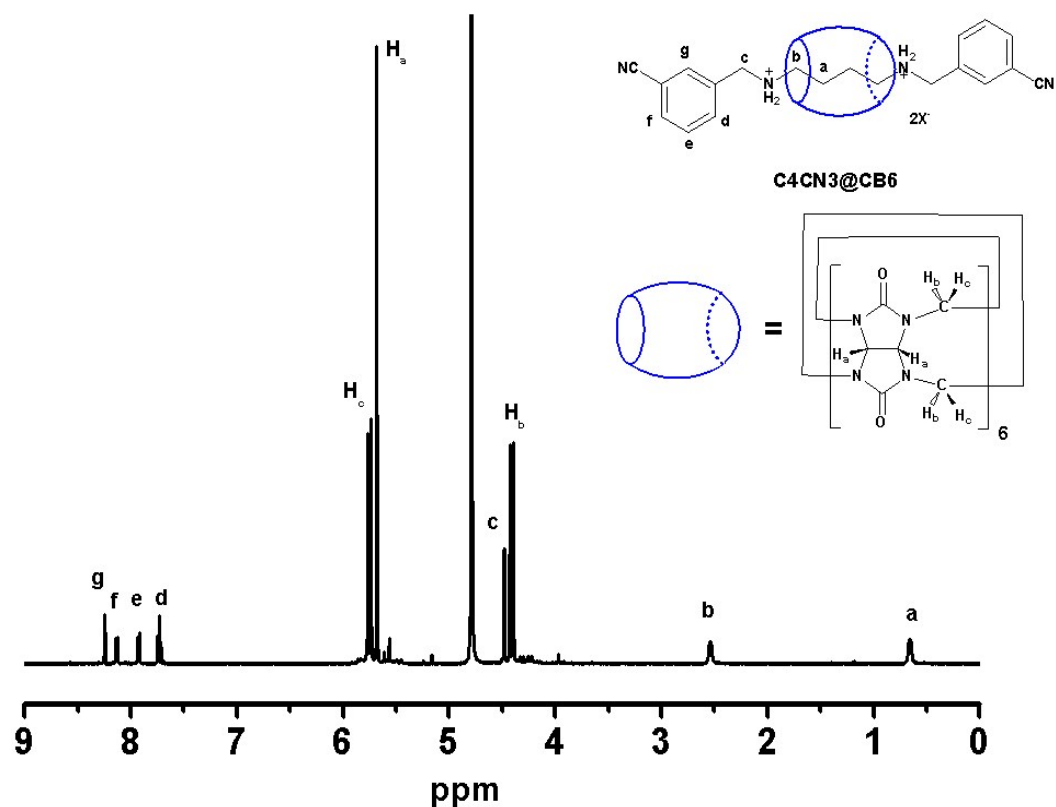


Figure S1. ^1H NMR spectrum of C4CN3@CB6 (500 MHz in D_2O)

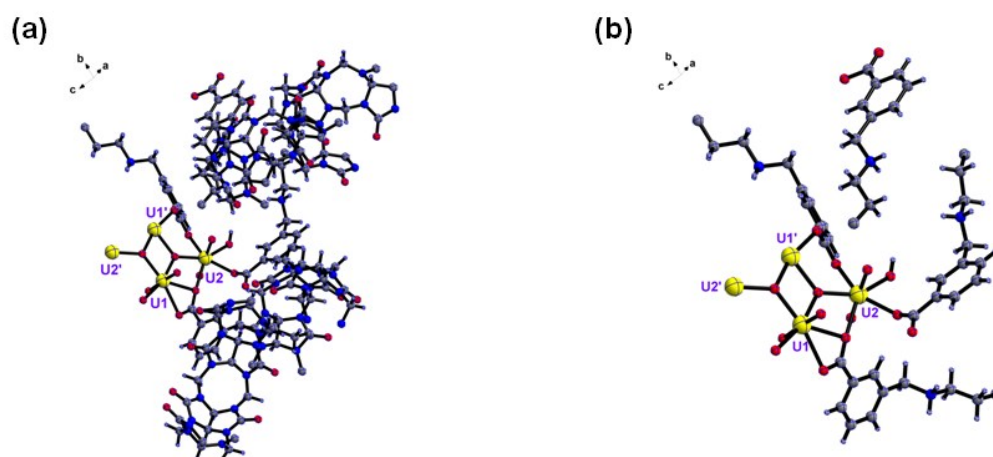


Figure S2. Crystallographic structure of **IHEP-URCP-2**: (a) ORTEP drawing of the asymmetric unit; (b) the asymmetric unit with all the cucurbituril macrocyclic moieties omitted for clarity.

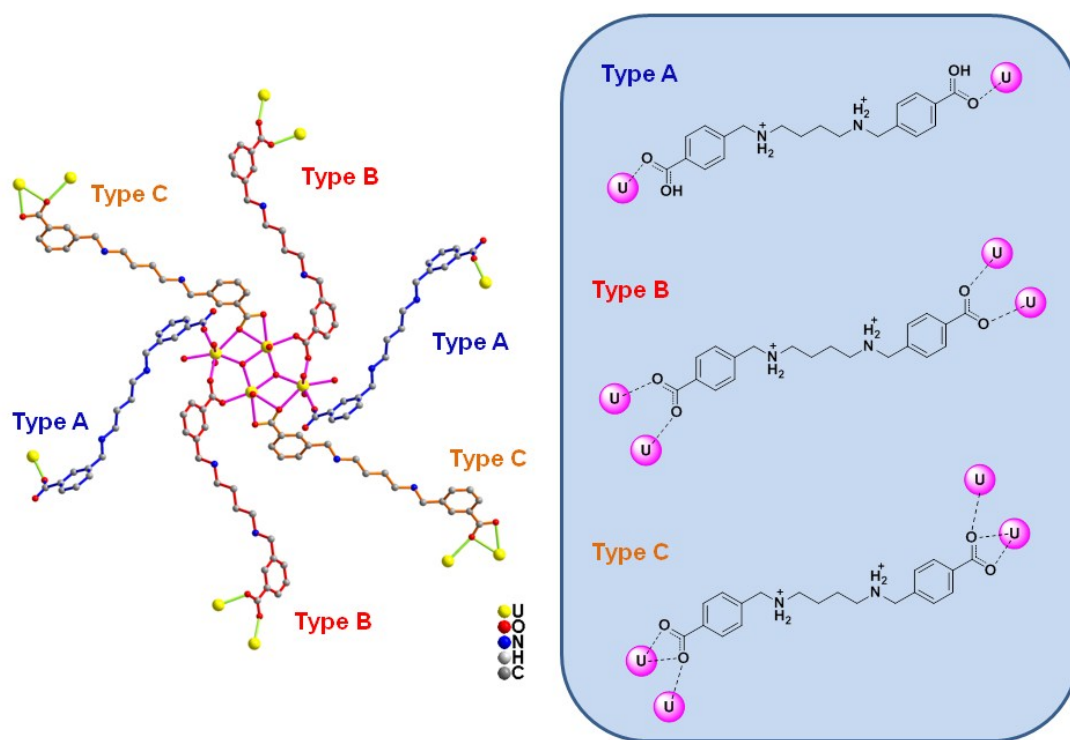


Figure S3. Three types of C4CA3@CB6 moieties in **IHEP-URCP-2**: C4CA3@CB6 with both ends in η^1 -mode corresponds to type A, that in $\mu_2\text{-}\eta^1\text{:}\eta^1$ -mode is type B, and that in $\mu_2\text{-}\eta^1\text{:}\eta^2$ -mode is type C.

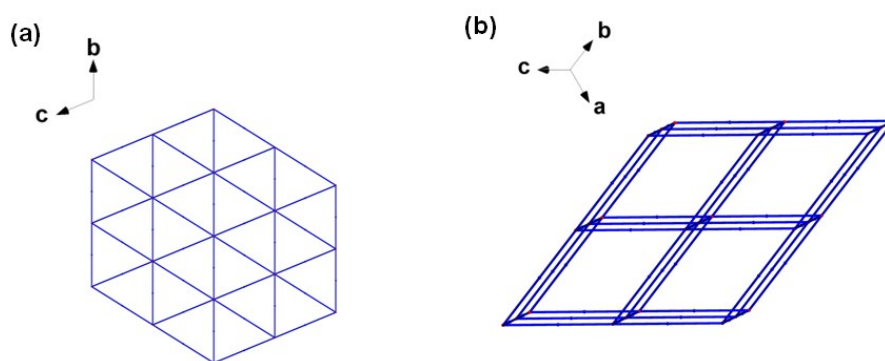


Figure S4. The α -polonium-like topology of the 3D uranyl polyrotaxane framework in **IHEP-URCP-2** viewed from different directions.

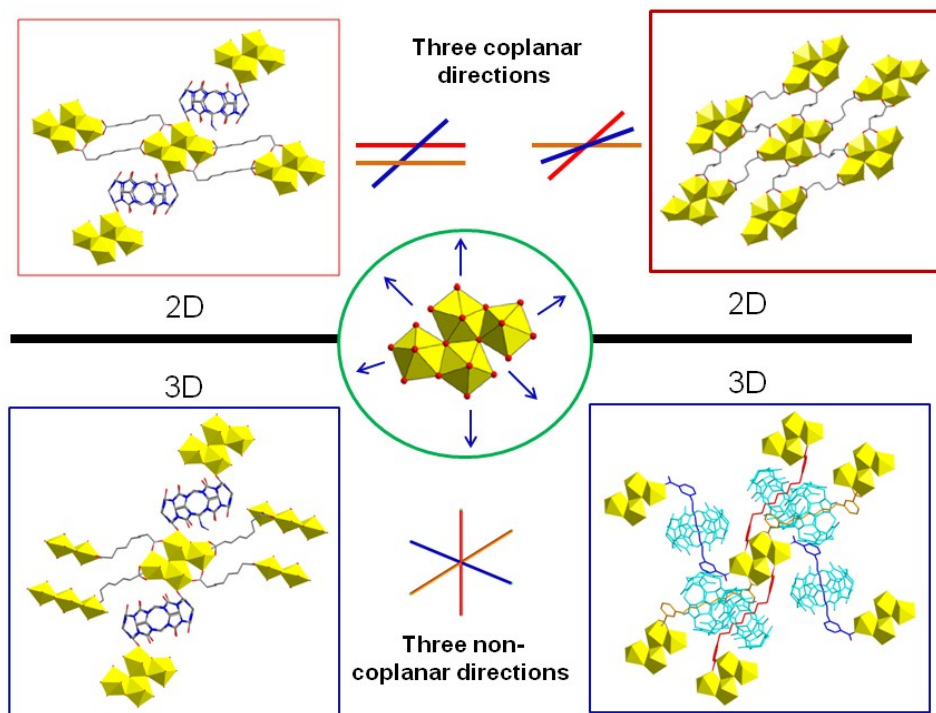


Figure S5. For 6-connected tetra-nuclear uranyl SBUs, all the six linkers extending to three different non-coplanar directions could afford three-dimensional frameworks, while those in coplanar directions only give 2D networks.

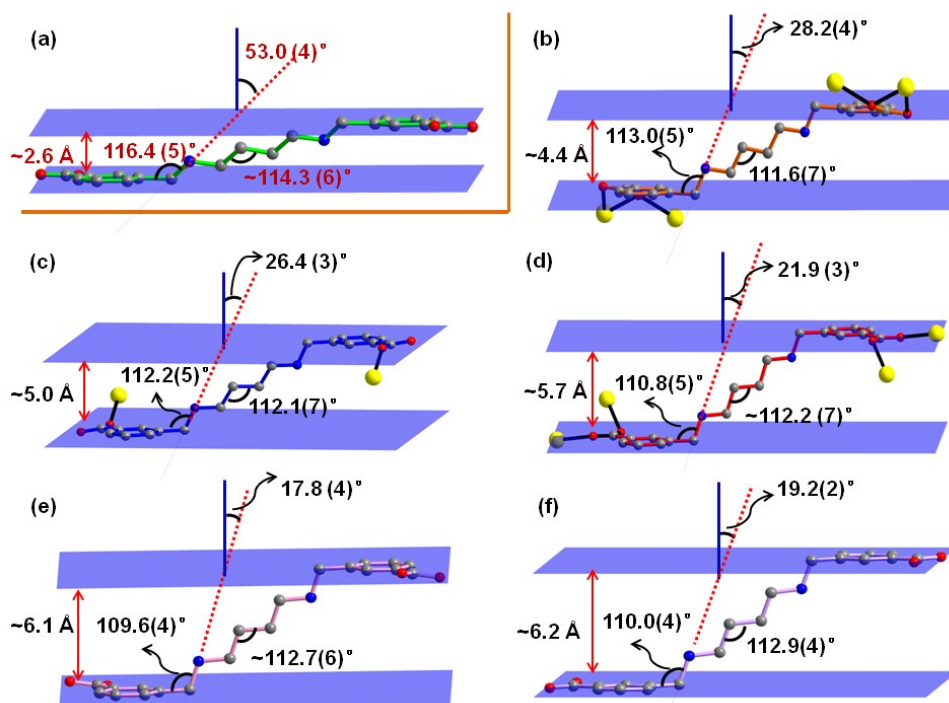


Figure S6. Comparison of molecular structures and configurations of **C4CA3** chain between (a) free pseudorotaxane of **IHEP-URCP-2**, (b-d) coordinated pseudorotaxane of **IHEP-URCP-2** and (e-f) simple precursors of **C4CA3@CB6**.

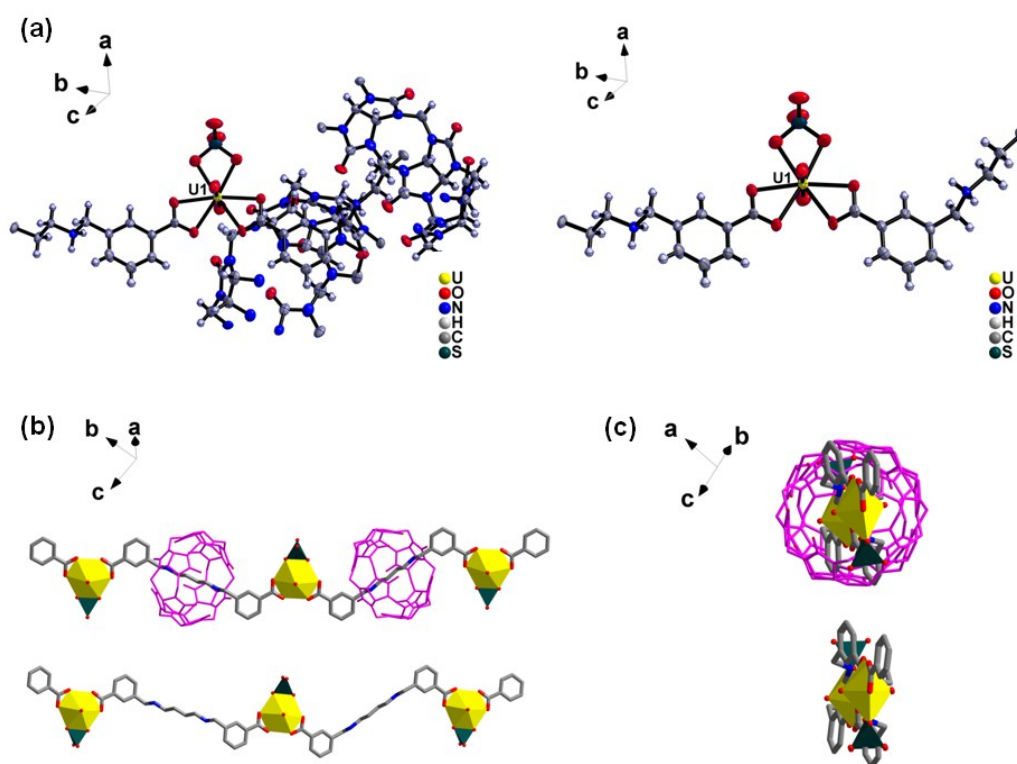


Figure S7. Crystallographic structure of **IHEP-URCP-3**: (a) ORTEP drawing of the asymmetric unit; (b) the asymmetric unit with all the cucurbituril macrocyclic moieties omitted for clarity; (c) the chain-like structure of **IHEP-URCP-3**; (d) the chain-like structure of **IHEP-URCP-3** viewed from another direction.

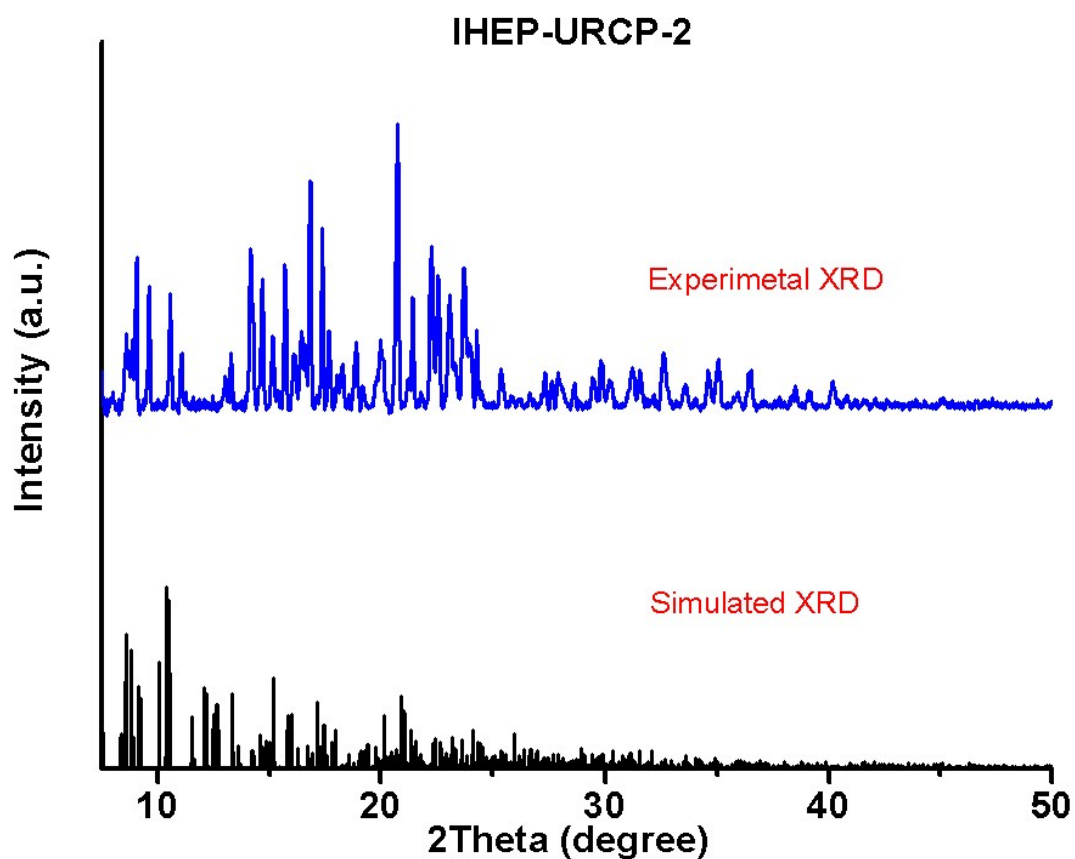


Figure S8. Powder X-ray diffraction pattern (PXRD) of **IHEP-URCP-2**. The upper and lower parts are experimental spectrum and simulated spectrum based on single crystal data, respectively.

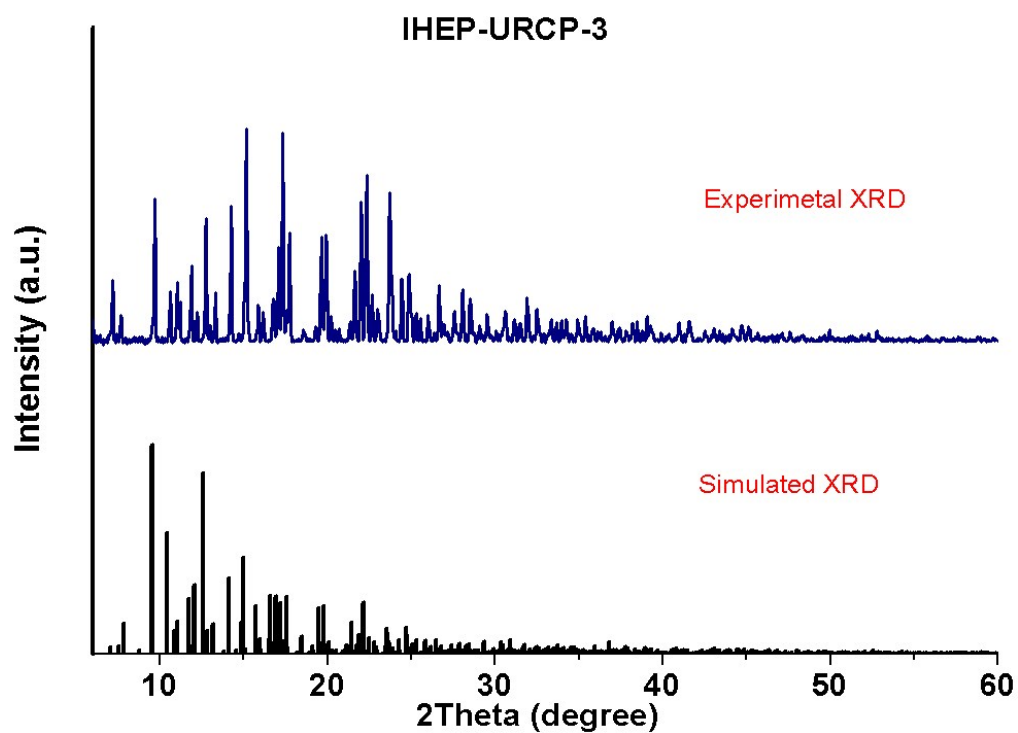


Figure S9. Powder X-ray diffraction pattern (PXRD) of **IHEP-URCP-3**. The upper and lower parts are experimental spectrum and simulated spectrum based on single crystal data, respectively.

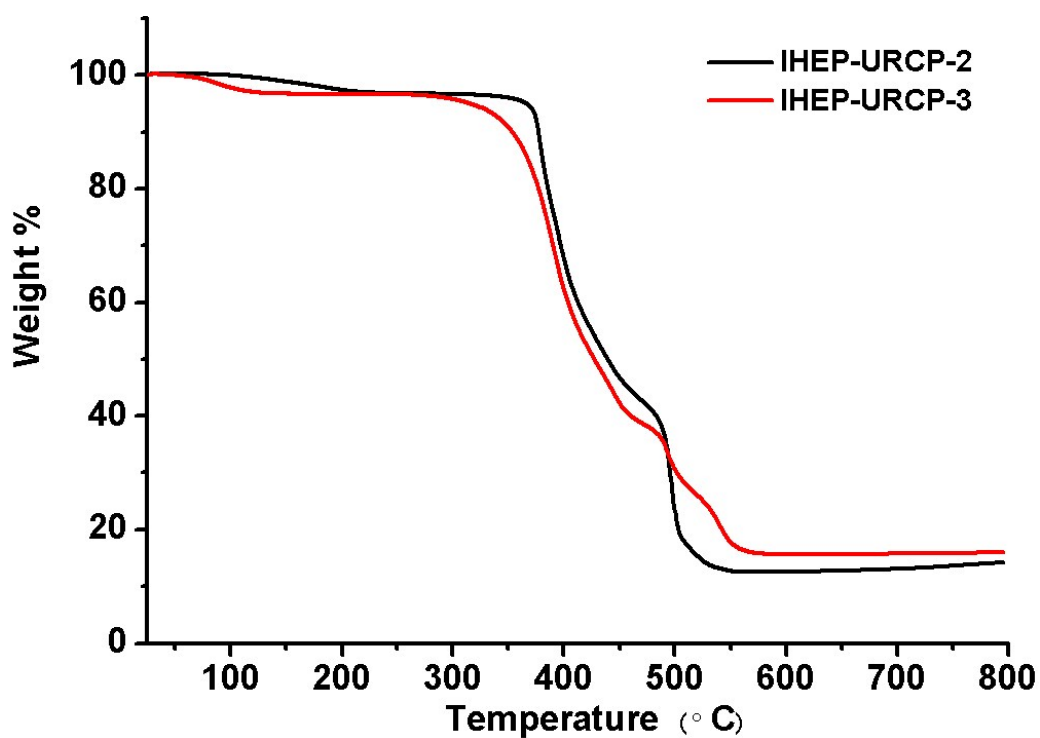


Figure S10. Thermogravimetric results of IHEP-URCP-2 and IHEP-URCP-3.

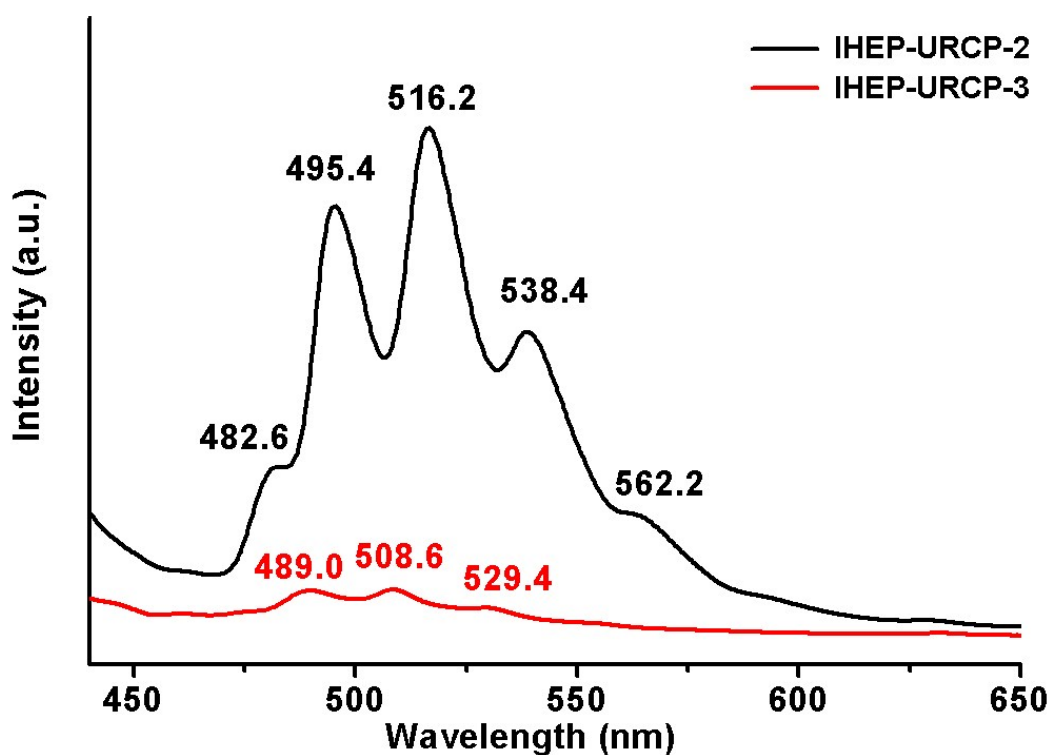


Figure S11. Fluorescence spectra of IHEP-URCP-2 and IHEP-URCP-3.

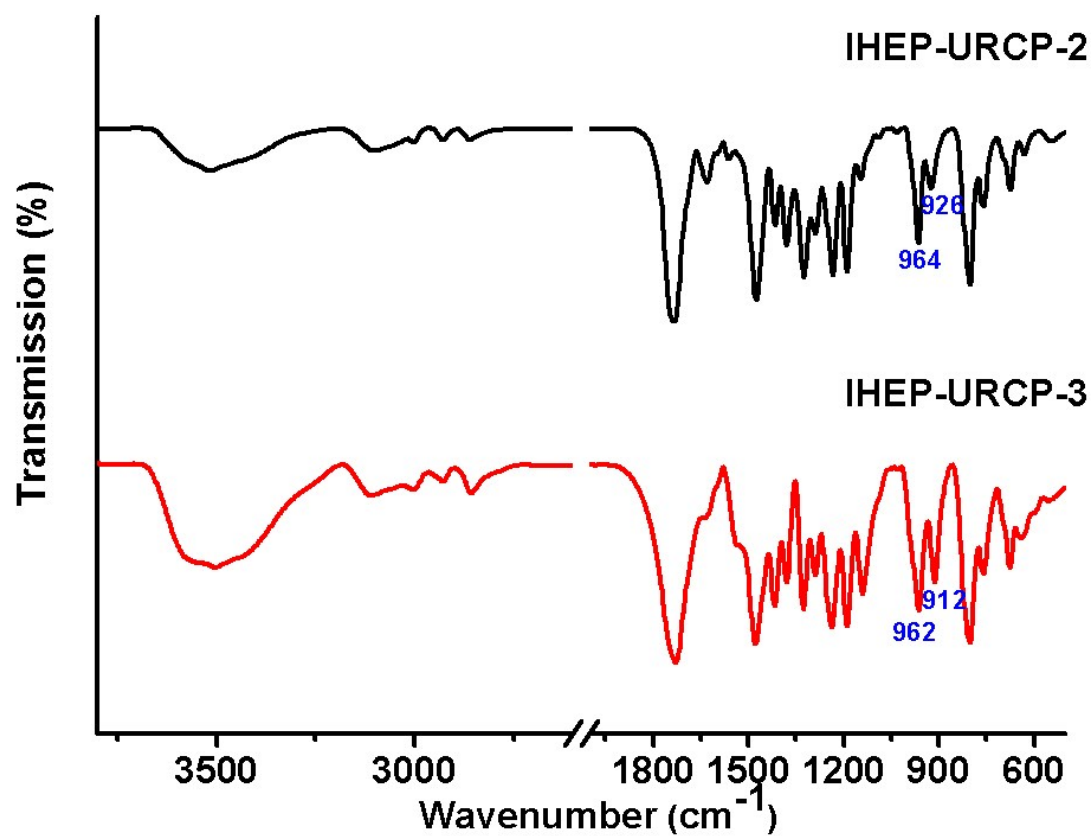


Figure S12. IR spectra of IHEP-URCP-2 and IHEP-URCP-3.

S2. Typical Tables

Table S1. Selected bond distances (Å) and bond angles (°) related to uranyl centers in **IHEP-URCP-2** and **IHEP-URCP-3**.

IHEP-URCP-2			
U(1)-O(1)	1.776(4)	U(2)-O(3)	1.766(5)
U(1)-O(2)	1.766(4)	U(2)-O(4)	1.774(4)
U(1)-O(5)	2.295(3)	U(2)-O(5)	2.224(3)
U(1)-O(5')	2.263(4)	U(2)-O(6)	2.595(3)
U(1)-O(6)	2.504(3)	U(2)-O(8)	2.286(4)
U(1)-O(7)	2.533(4)	U(2)-O(10)	2.436(4)
U(1)-O(11)	2.374(4)	U(2)-O(1W)	2.455(4)
O(1)-U(1)-O(2)	174.7(2)	O(3)-U(2)-O(4)	174.0(2)
IHEP-URCP-3			
U(1)-O(1)	1.781(5)	U(1)-O(5)	2.487(5)
U(1)-O(2)	1.759(5)	U(1)-O(6)	2.452(5)
U(1)-O(3)	2.471(5)	U(1)-O(7)	2.438(6)
U(1)-O(4)	2.468(5)	U(1)-O(8)	2.474(5)
O(1)-U(1)-O(2)	178.6(2)		
